Journal of Molecular Liquids 366 (2022) 120156

Contents lists available at ScienceDirect

Journal of Molecular Liquids

journal homepage: www.elsevier.com/locate/molliq

In silico study of liquid crystalline phases formed by bent-shaped molecules with excluded volume type interactions

Piotr Kubala [a], Wojciech Tomczyk [a,b,*], Michał Cieśla [a]

[a] Institute of Theoretical Physics, Jagiellonian University, Łojasiewicza 11, 30-348 Kraków, Poland
[b] Jerzy Haber Institute of Catalysis and Surface Chemistry, Polish Academy of Sciences, Niezapominajek 8, 30-239 Kraków, Poland

ARTICLE INFO

Article history:
Received 3 February 2022
Revised 16 July 2022
Accepted 19 August 2022
Available online 24 August 2022

Keywords:
Monte Carlo simulations
Molecular dynamics simulations
Liquid crystals
Bent-shaped molecules
Twist-bend nematic
Mirror symmetry breaking

ABSTRACT

What impact does the mesogens' shape have on the formation of the liquid crystalline phase? Using Monte Carlo and molecular dynamics simulations we numerically studied a liquid composed of achiral, bent-shaped molecules built of tangent spheres. The system is known to spontaneously break mirror symmetry, as it forms a macroscopically chiral, twist-bend nematic phase [Phys. Rev. Lett. **115**, 147801 (2015)]. We examined a full phase diagram by altering the molecules' curvature along with packing fractions and observed several phases characterized by the orientational and/or translational ordering of molecules. Apart from conventional nematic, smectic A, and the aforementioned twist-bend nematic phase, we identified splay-bend smectic phase. For large densities and strongly curved molecules, another smectic phase emerged, where the polarization vector rotates within a single smectic layer.

1. Introduction

Comprehension of the spontaneous mirror symmetry breaking (SMSB) phenomenon is essential for understanding fundamental aspects such as life itself [1–3]. Investigations revolving around the origins and corollary of SMSB stand simultaneously at the forefront and frontiers of contemporary soft matter science [4,5]. One of the playgrounds to investigate the nature of SMSB are liquid crystals (LCs), where supramolecular chiral and polar structures are assembled from achiral, bent-shaped (curved) molecules [6,7]. Bent-shaped molecules (BSMs) tend to form various phases, including smectics and nematics [8–10]. The latter, however, has recently experienced a resurgence of worldwide interest. It happened because of the discovery of twist-bend nematic (N_{TB}) phase [11–14], which constitutes the first example of SMSB in a liquid state with no support from long-range spatial ordering. The characteristic feature of N_{TB} is the emergence of heliconical (1D modulated) structure of nanoscale pitch ($p \approx 8 - 10$ nm) with a ground-state exhibiting a degenerate sign of chirality (ambidextrous chirality), which means that both helix handedness, either right or left, are equiprobable (Fig. 1). In no time, it turned out that one of the essential prerequisites for the stabilization of N_{TB} are "adequately curved" molecules [15–17] in line with Meyer's [18] and Dozov's [19] conjecture. However, there is still an ongoing debate concerning the N_{TB}'s structure and properties [20,21]. Further advances in the studies of N_{TB} subsequently sprouted into a broad sub-field of liquid crystal research dedicated to novel nematic phases of non-standard symmetries [22–25].

It is noteworthy to point out that remarkable features of nematic phases formed by BSMs are not limited solely to the phenomenon of SMSB. The list is vast but just to name a few [29,9]: unusual hierarchy of elastic constants, giant flexoelectricity, non-standard dielectric, and rheological behaviours. The BSMs are also said to be the perfect candidates for optically biaxial liquid, namely biaxial nematic (N_B), predicted by Freiser in 1970 [30]. They owe it to the introduction of the "kink" in the molecular structure which naturally specifies a secondary direction perpendicular to the long molecular axis, for orientational ordering [31,32].

All the above makes LCs formed by BSMs, *per se*, a riveting field to explore both from experimental and theoretical points of view (see, e.g., [33–36,9,37,27,28] and references therein). In particular, substantial efforts were undertaken to decipher how the molecule's structure influences the emergence of individual mesophases [38,39,32]. One of valuable tools in such studies are computer simulations, such as Monte Carlo (MC) sampling and Molecular Dynamics (MD), which have a long-standing tradition in the investigation of structural properties of LC phases using a diverse range of models ranging from simplified lattice systems

* Corresponding author at: Institute of Theoretical Physics, Jagiellonian University, Łojasiewicza 11, 30-348 Kraków, Poland.
E-mail address: wojciech.tomczyk@ikifp.edu.pl (W. Tomczyk).

https://doi.org/10.1016/j.molliq.2022.120156
0167-7322/

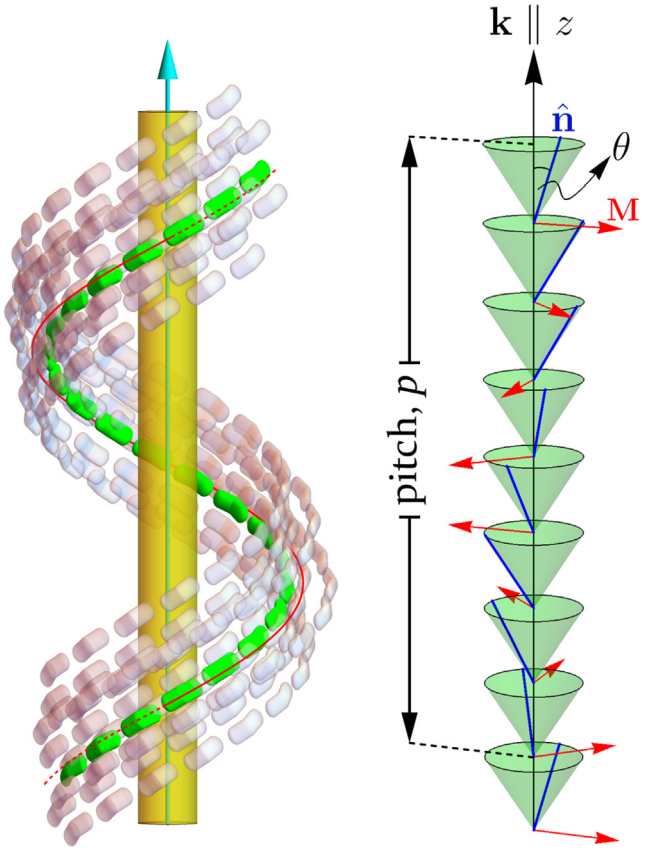

Fig. 1. Schematic depiction of the twist-bend nematic phase characterized by the finite pitch p and heliconical tilt angle θ $(0 < \theta < \pi/2)$ between the director $\hat{\mathbf{n}}$ and the wavevector $\mathbf{k} \parallel z$ ($\mathbf{k} = k\hat{\mathbf{z}} = (2\pi/p)\hat{\mathbf{z}}$). The polarization $\mathbf{M}$, where $\mathbf{M} \parallel \hat{\mathbf{n}} \times \mathbf{k}$, is precessing around $\mathbf{k}$ along with $\hat{\mathbf{n}}$. Spontaneous mirror symmetry breaking in the twist-bend nematic phase, arising from chiral conformations of achiral molecules (ones lacking stereogenic center), leads to the ground-state with doubly degenerate handedness. Namely, each chiral conformer has its mirror counterpart differing in sign of chirality, which results in twin domains of opposite (left- and right-) handedness [26,16]. (Left) Adapted from Ref. [27] with permission from the Royal Society of Chemistry. (Right) Adapted from Ref. [28] published under ACS AuthorChoice with CC-BY license.

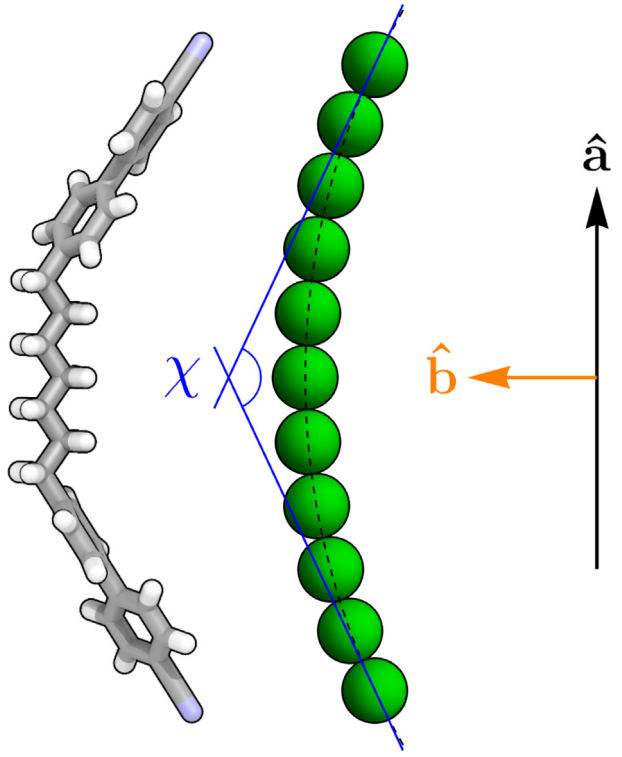

Fig. 2. Left: Molecular structure of N_{TB} forming mesogen CB7CB [11] rendered via QuteMol [63]. Right: Model bent-shaped molecule with C_{2v} symmetry composed of eleven tangent spheres whose centers are equidistantly distributed on the arc. The bend angle χ is defined as the angle formed by two lines, tangent to the arc at the centers of end-point spheres. Please note that in this convention, the higher the bend angle, the smaller is molecule's curvature (it is less bent). Unit vectors $\hat{\mathbf{a}}$ and $\hat{\mathbf{b}}$ define the molecular reference frame, where $\hat{\mathbf{a}}$ equates with the molecular long axis and $\hat{\mathbf{b}}$ is parallel to the molecule's twofold (C_2) symmetry axis.

to fully atomistic ones [40–42]. Generally, but not limited to, the anisotropic shape of BSMs can be approximated in the simulations either by V-like or C-like shaped objects (reflecting the C_{2v} symmetry) composed of, e.g., needles [43–45], spheres [46–50], or spherocylinders [51–56]. It has been shown that those systems, each one separately, produce a richness of interesting nematic and smectic phases. However, especially appealing are the systems where the supramolecular chirality emerges out of pure entropy-driven interactions [49,57]. To our best knowledge, there is a modest number of works focused on computer simulations of N_{TB} and its structurally-related counterparts [58,59,13,49,55,56,60–62].

Herein, we extended the work of Greco and Ferrarini [49] where it was shown that for a model system of BSMs, composed of eleven tangent spheres (see Fig. 2), it is possible to observe the stabilization of N_{TB} arising from the packing entropy in MD simulations. We aim to provide an in-depth analysis of this system by altering the BSMs' curvature and packing fractions in order to obtain the full phase diagram for the liquid state[1]. To achieve it, we performed both MC and MD simulations.

The article is organized as follows. In Section 2 the system under study is described together with the details concerning the MC and MD simulations used to investigate its properties. The results of the simulations are given in Section 3 where they are compared with the current literature. In Section 4 we provide conclusions drawn from the acquired data.

2. Model and simulation details

2.1. The model system

BSMs were modeled by eleven tangent spheres of diameter σ placed on a circular arc with a variable bend angle χ (see Fig. 2). For $\chi = 180^\circ$, the molecule reduces to a linear chain of tangent spheres, while for $\chi = 0^\circ$ it forms a semi-circle. To study lyotropic phase transitions in a system composed of such molecules, we examined two types of excluded-volume interaction. The first one is hard-core interaction [64], while the second is Weeks-Chandler-Andersen (WCA) [65,66] soft repulsion, defined as

$$U(r_{mn}) = \begin{cases} 4\varepsilon\left[\left(\frac{\sigma}{r_{mn}}\right)^{12} - \left(\frac{\sigma}{r_{mn}}\right)^{6}\right] + \varepsilon & \text{if } r_{mn} < 2^{1/6}\sigma \\ 0 & \text{if } r_{mn} \geq 2^{1/6}\sigma, \end{cases} \quad (1)$$

where r_{mn} is the distance between the interaction centers and ε is the energy scale. The free parameters of the model (σ, ε) can be conveniently incorporated into the reduced pressure $P^* = P\sigma^3/\varepsilon$ and reduced temperature $T^* = k_B T/\varepsilon$. For hard-core repulsion, the equation of state depends only on a single parameter – the $P^*/T^* = P\sigma^3/(k_B T)$ ratio [67,64]. For WCA interaction the system is sensitive to P^* changes, while the dependence on T^* is weak [68]. The emergent phases were studied as a function of bend angle χ

[1] The study of regions, where crystal structures emerge is outside of the article's scope and stands as the starting point for further research.

and packing fraction η. The latter is a natural parameter for lyotropic systems and enables us to compare the two interaction models [68]. For both of them, the main contribution to Helmholtz free energy is the packing entropy: $F \approx -TS$ (the formula is exact for hard-core repulsion), so the phases with the highest entropy minimize F and thus are promoted.

2.2. Simulation methods

The hard-core interactions were simulated using Monte Carlo sampling in *NPT* ensemble [69] for $P^*/T^* \in [0.2, 2.0]$. The system was built of $N = 3000$ molecules. For a selected set of parameters giving periodic phases, simulation was repeated for $N = 6000$ and double the box size to ensure that the finite size effects are not present. A single MC cycle consisted of N molecule moves and a volume move. To perform a molecule move, a single molecule was sampled at random. Then, the molecule was translated by a random vector and rotated by a random angle around a random axis. The move was accepted provided it did not introduce an intersection. For volume moves all three lengths of an orthorhombic simulation box with periodic boundary conditions and the positions of molecules were scaled by three independent logarithmically distributed factors. Moves introducing overlaps were rejected and the rest of them was accepted according to Metropolis criterion. Anisotropic scaling was chosen to avoid frustration, which could introduce a bias in the period of emergent structures. The extents of random moves were selected such that the acceptance ratio was around 15%. The initial configuration was a diluted antiferroelectric sc crystal, which was then compressed or expanded to a target density. The equilibration was very sluggish due to the concavities of molecules and required up to 2×10^8 of full MC cycles. The production runs to sample ensemble averages consisted of 3×10^7 cycles. To accelerate the simulations, we parallelized them using domain division [70].

The MD simulations of $N = 2025$ molecules, interacting via the WCA potential in the *NPT* ensemble at various values of the pressure P^* in the interval $0.2 \leqslant P^* \leqslant 2.0$, were performed using the open-source software LAMMPS [71]. All relevant simulation aspects were set up according to the framework provided in [72]. Equilibration and production runs were conducted for 10^7 timesteps each.

Within both simulation schemes, i.e., MC and MD, we examined particles with a fixed bend angle $\chi \in [90°, 180°]$.

2.3. Order parameters

Distinctive features of a particular phase can be characterized by appropriate order parameters and the corresponding degree of ordering. In nematic and smectic phases, the molecules' long axes (denoted as $\hat{\mathbf{a}}$, see Fig. 2) tend to orient, on average, along a preferred direction called the director $\hat{\mathbf{n}}$ ($\hat{\mathbf{n}}^2 = 1$) [73]. Such kind of alignment can be quantified by the second-rank order parameter [74]:

$$\langle P_2 \rangle = \frac{1}{N} \langle \sum_{i=1}^{N} P_2(\hat{\mathbf{a}}_i \cdot \hat{\mathbf{n}}) \rangle, \tag{2}$$

where the sum is over all N molecules in the system, $P_2(\dots)$ is the Legendre polynomial of degree 2, $\hat{\mathbf{a}}_i$ is a molecular axis vector of i-th molecule (cf. Fig. 2) and $\langle \dots \rangle$ denotes the time average over uncorrelated system snapshots. If $\langle P_2 \rangle = 0$ orientations are isotropic, $\langle P_2 \rangle = 1$ is a perfect order, and for $\langle P_2 \rangle = -1/2$ all molecules are perpendicular to $\hat{\mathbf{n}}$. Alternatively, $\langle P_2 \rangle$ can be computed by diagonalising the second rank $\mathbf{Q}$-tensor [74]

$$Q_{\alpha\beta} = \frac{1}{N} \sum_{i=1}^{N} \frac{3}{2} \left(\hat{a}_{i,\alpha} \hat{a}_{i,\beta} - \frac{1}{3} \delta_{\alpha\beta} \right), \tag{3}$$

where $\hat{a}_{i,\alpha}$ and $\hat{a}_{i,\beta}$ are the Cartesian components of $\hat{\mathbf{a}}_i$ and $\delta_{\alpha\beta}$ is the Kronecker delta. The nematic order parameter P_2 (for a single snapshot) is associated with the largest-modulus of a non-degenerate eigenvalue of $\mathbf{Q}$ and $\hat{\mathbf{n}}$ is the corresponding eigenvector. In this formulation, zero-energy diffusive motion of $\hat{\mathbf{n}}$ does not have effect on $\langle P_2 \rangle$'s value.

The density modulation is measured by smectic order parameter [73]:

$$\langle \tau \rangle = \frac{1}{\rho} \left\langle \left| \sum_{i=1}^{N} \exp(\mathrm{i}\mathbf{k} \cdot \mathbf{r}_i) \right| \right\rangle, \tag{4}$$

where ρ is number density, $\mathbf{k}$ is a wavevector of density undulation and $\mathbf{r}_i$ are molecules' centers of mass. Typically, for non-tilted smectic phases $\mathbf{k} \parallel \hat{\mathbf{n}}$. For $\langle \tau \rangle = 0$ there is no density modulation, whereas for $\langle \tau \rangle = 1$ the molecules form perfect layers with a spacing equal to $2\pi/|\mathbf{k}|$. In simulations, $\mathbf{k}$ has to be compatible with periodic boundary conditions. It can be achieved by taking a linear combination of reciprocal box vectors with integer coefficients h, k, l (Miller indices) [75]. To find an optimal wavevector, we tested all combinations of $h, k, l \in [-5, 5]$ and selected the ones giving the highest value of τ. Using this method one can avoid assuming $\mathbf{k}$ *a priori*.

Total polarization can be computed as a sum of molecule polarization vectors

$$\langle \mathbf{M} \rangle = \langle \sum_{i=1}^{N} \hat{\mathbf{b}}_i \rangle. \tag{5}$$

As it will be seen from the results, the non-zero polarization can be present when one restricts the summation to a plane perpendicular to $\hat{\mathbf{n}}$, however, at the same time, it can vary in the direction of $\hat{\mathbf{n}}$ and give zero net polarization when summed over the whole system. To account for such variations, one can calculate the norm $M(C_j) = ||\mathbf{M}(C_j \pm \Delta C/2)||$ for molecules in a narrow shell between two planes $\mathbf{r} \cdot \hat{\mathbf{n}} = C_j \pm \Delta C/2$ and sum them over the whole system:

$$\langle m \rangle = \frac{1}{N_b} \langle \sum_{j=1}^{N_b} M(C_j) \rangle, \tag{6}$$

where $N_b = L/\Delta C$ is the number of shells and L is the system length in the direction of $\hat{\mathbf{n}}$.

An additional insight into the phase structure can be provided by pair correlation functions [76] (for the $\hat{\mathbf{a}}$ and $\hat{\mathbf{b}}$ vectors, cf. Fig. 2) measured with reference to z-axis:

$$S_{aa}^{220}(R_z) = \langle \frac{3}{2} \left(\hat{\mathbf{a}}_i \cdot \hat{\mathbf{a}}_j - \frac{1}{3} \right) \rangle_{ij}, \tag{7}$$

$$S_{bb}^{110}(R_z) = \langle \hat{\mathbf{b}}_i \cdot \hat{\mathbf{b}}_j \rangle_{ij}, \tag{8}$$

$$S_{aa}^{221}(R_z) = \langle \left[(\hat{\mathbf{a}}_i \times \hat{\mathbf{a}}_j) \cdot \hat{\mathbf{z}}_{ij} \right] (\hat{\mathbf{a}}_i \cdot \hat{\mathbf{a}}_j) \rangle_{ij}. \tag{9}$$

Here, $\langle \dots \rangle_{ij}$ denotes the averaging over all pairs of molecules, whose mass centers' z coordinates differ by $R_z \pm \Delta R_z/2$ (ΔR_z corresponds to numerical bin size) in a single, final snapshot of the system, and $\hat{\mathbf{z}}_{ij}$ is z axis unit vector, pointing from j-th to i-th molecule. $S_{aa}^{220}(R_z)$ parameter measures nematic-like correlations of molecules' main axes $\hat{\mathbf{a}}$, S_{bb}^{110} quantifies the correlation of polarization axes $\hat{\mathbf{b}}$, while S_{aa}^{221} is sensitive to chirality of the structure.

3. Results

3.1. Phase overview

The system exhibits a variety of liquid phases: isotropic liquid (Iso), nematic (N), twist-bend nematic (N_{TB}), non-polar smectic A (SmA), splay-bend smectic (Sm_{SB}) and an unidentified polar smectic (SmX). The phase diagram for hard-core interactions is shown in Fig. 3. WCA soft repulsion recreates all the phases with nearly identical phase borders. All order parameters described by Eq. (2), (4) and (6) are gathered in Fig. 4 as a function of the bend angle χ and the packing fraction η. Finally, system snapshots for all identified phases are depicted in Fig. 5.

For each value of χ and sufficiently low η, the molecules form ordinary isotropic liquid as shown by low values of all order parameters indicating a lack of any long-range correlations (see Fig. 5(a)). Around $\eta = 0.45$ the system crystallizes into several types of hexagonal close-packed crystals, which is beyond the scope of this work. The boundary of the Iso phase moves upwards in η for a decreasing bend angle χ. It can be explained by the fact, that a smaller bend angle results in less prolate molecules, for which the entropic gain from orientational ordering is lower.

3.2. Nematic phases

The ordinary nematic phase N can be observed for $\chi > 110^\circ$, as indicated by a sharp jump of $\langle P_2 \rangle$ value from near zero to over 0.5 on the phase boundary and lack of density modulation (Fig. 5(b)). A growing η results in an increase of $\langle P_2 \rangle$ to almost 0.9 for $\chi \approx 180^\circ$, which is significantly higher than a typical range $[0.3, 0.7]$ for nematics observed in experiments [77]. Additionally, two smallest eigenvalues of $\langle \mathbf{Q} \rangle$ are comparable, which together with a vanishing net polarization $\langle \mathbf{M} \rangle \approx \mathbf{0}$ (result not shown) indicates that the nematic phase is uniaxial. Layer polarization $\langle m \rangle$ is also close to zero, which means that the phase is homogeneous.

The situation changes for a phase forming over the Iso phase for $\chi < 110^\circ$ and over the N phase in the range $\chi \in [110^\circ, 140^\circ]$, for η values between 0.29 and 0.35 (Fig. 5(c)). No density modulation suggests that is a nematic-like phase, however with $\langle P_2 \rangle \in [0.3, 0.5]$, lower than for the ordinary N phase in the system. The net polarization is zero, while $\langle m \rangle$ lies in the range $[0.4, 0.8]$, indicating high polar ordering in planes perpendicular to $\hat{\mathbf{n}}$. A closer inspection (Fig. 6) reveals that this is N_{TB} phase [58,59,49,56]. Assuming the global director is aligned with the z axis (cf. Fig. 1), the director $\hat{\mathbf{n}}$ can be parameterized as

$$\hat{\mathbf{n}}(x, y, z) = \begin{pmatrix} \sin(\theta)\cos(2\pi z/p) \\ \sin(\theta)\sin(2\pi z/p) \\ \cos(\theta) \end{pmatrix}. \tag{10}$$

The spatial dependence of $\mathbf{M}$ is similar, with $\mathbf{M} \perp \hat{\mathbf{n}}$. The pitch and tilt angle vary in phase space – $p \in [25\sigma, 45\sigma]$ and $\theta \in [25^\circ, 35^\circ]$, respectively. With increasing packing fraction η or decreasing bend angle χ the pitch shortens and tilt angle becomes more obtuse. Spatial variations of $\hat{\mathbf{n}}$ and $\mathbf{M}$ fields are reflected by $S^{KKL}_{\alpha\alpha}$ correlation functions plotted in Fig. 6(a) for two sets of parameters: $(\chi, \eta) = (130^\circ, 0.32)$ and $(\chi, \eta) = (100^\circ, 0.33)$. They all have the same period p as the director field. For $\chi = 130^\circ$, S^{220}_{aa} reaches a maximal value 0.8 at $R_z = 0 \equiv p$ indicating a high local nematic order (compared to a global $\langle P_2 \rangle \approx 0.4$ value). In between the maxima, it falls until it reaches the minimal value of -0.3 for $R_z = p/2$ when local preferred directions of long molecular axes have an opposite tilt. The S^{110}_{bb} function follows a sinusoidal pattern, which can be predicted assuming the polarization field rotates in the xy plane. Notice that the amplitude is lower than 1, namely, S^{110}_{bb} reaches ± 0.5. It

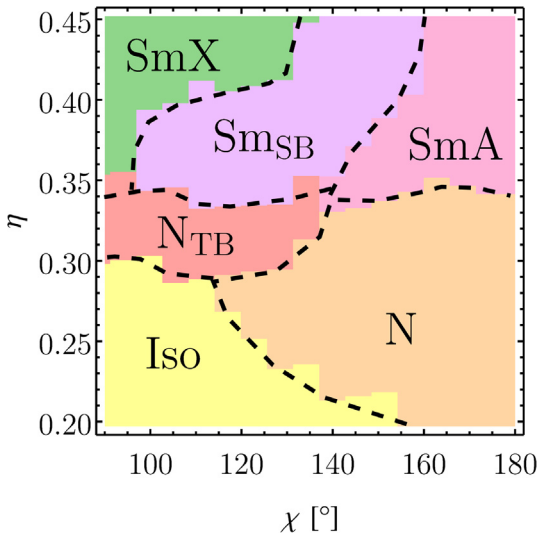

Fig. 3. Phase diagram for hard-core interactions in (χ, η) parameters space. The following phases are present: isotropic liquid (Iso), nematic (N), twist-bend nematic (N_{TB}), non-polar smectic A (SmA), splay-bend smectic (Sm_{SB}) and unidentified polar smectic (SmX). Black dashed lines are arbitrarily drawn to visually separate the phases' regimes. For $\chi \in [90^\circ, 180^\circ]$ and $\eta < 0.35$ the phase sequences are in line with the results from the mean-field theory [37,27].

suggests, that vectors $\hat{\mathbf{b}}$ have a local spread. A non-zero value of S^{221}_{aa} confirms that the director field is chiral. For a smaller bend angle, i.e. $\chi = 100^\circ$, all correlation functions are qualitatively identical, however, one can see some quantitative differences. S^{221}_{aa} parameter remains unchanged. S^{220}_{aa} has a comparable maximal value meaning that a local nematic order is similar, however, the minimum is broader and of a higher magnitude, which is expected for a wider tilt angle θ. At the same time, the amplitude of S^{110}_{bb} increases to 0.7 suggesting a lower local spread of molecules' polarization vectors. It is confirmed by a higher value of $\langle m \rangle$ for $\chi = 100^\circ$ bend angle compared to $\chi = 130^\circ$.

N_{TB} can be described using phenomenological lowest-order[2] Oseen-Zocher-Frank elastic free energy density [78–80]

$$F_{OZF} = \frac{1}{2}K_{11}[\hat{\mathbf{n}}(\nabla \cdot \hat{\mathbf{n}})]^2 + \frac{1}{2}K_{22}[\hat{\mathbf{n}} \cdot (\nabla \times \hat{\mathbf{n}})]^2 + \frac{1}{2}K_{33}[\hat{\mathbf{n}} \times (\nabla \times \hat{\mathbf{n}})]^2, \tag{11}$$

where subsequent terms represent, respectively, splay, twist, and bend deformations of director field and K_{ii} $(i = 1, 2, 3)$ are Frank elastic constants. All three Frank elastic constants have to obey Ericksen's inequalities [81], i.e.: $K_{ii} \geqslant 0$ $(i = 1, 2, 3)$, otherwise perfect alignment (homogeneous nematic) would not correspond to a state of minimum energy. However, if one were to consider a scenario where $K_{33} < 0$, then it would occur that bend deformation is energetically favorable and the reference state, namely a homogeneous nematic, becomes unstable [19]. As there does not exist a (two-dimensional) structure with constant bend without topological defects, it has to be combined with at least one of the other deformations, either splay or twist. If $K_{11}/K_{22} > 2$, then the frustration is diminished through escape into third dimension, which leads to the stabilization of twist-bend structure, whereas for $K_{11}/K_{22} < 2$ two dimensional splay-bend structure emerges [19]. As pointed out by Shamid *et al.* [59], the effective K_{33} constant can become negative below a certain critical temperature, when

[2] This is a valid approach that provides qualitative results but in order to reflect experimental data a more holistic method should be incorporated [28].

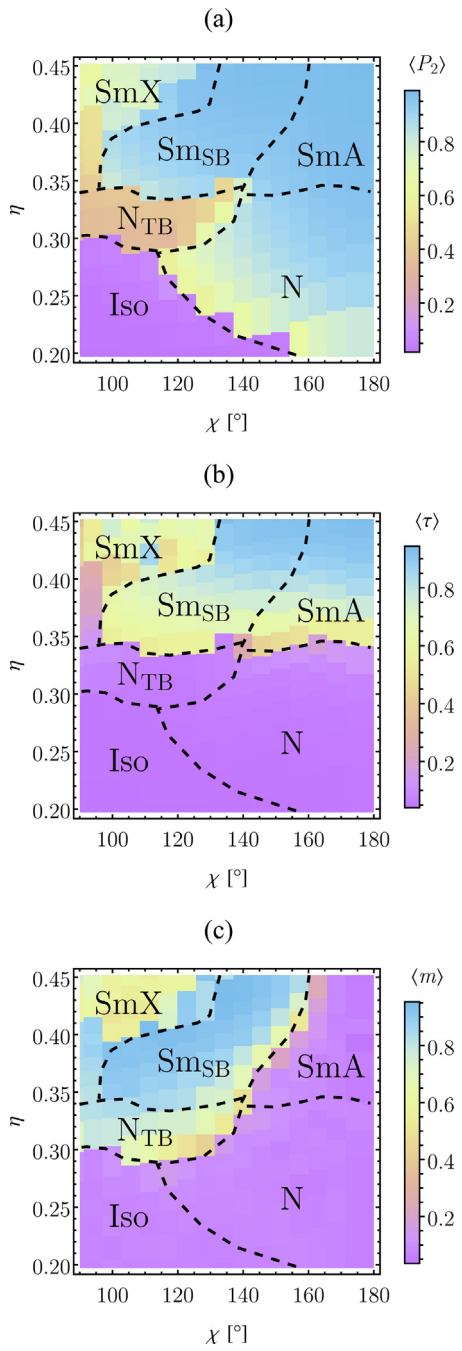

Fig. 4. Ensemble averages of order parameters as a function of χ and η. (a) Nematic order parameter $\langle P_2 \rangle$, (b) smectic order parameter $\langle \tau \rangle$ and (c) layer polarization $\langle m \rangle$.

the coupling of polarization with bend deformation is introduced, supporting the assumption that N_{TB} is inherently polar. The phase can be also understood through geometrical reasoning [37,82,27,28]. For curved spherocylinders, one can predict a correct relation between molecule bend angle, pitch p, and tilt angle θ matching the spherocylinder curvature with an integral curve of a director field $\hat{\mathbf{n}}$ [56].

3.3. Smectic phases

For $\eta > 0.34$, smectic phases are formed. The N phase is adjacent to an ordinary SmA phase – $\langle \tau \rangle$ is over 0.5 and strata are clearly visible [Fig. 5(d)]. Further compression narrows the spread of molecules' mass centers in the direction normal to the layer and τ approaches unity for a high η. Typically, $\langle P_2 \rangle$ value experiences a jump on the N-SmA boundary from around 0.4–0.6 to over 0.8 [58], however in some systems it is small or absent [52]. Here, no abrupt change of $\langle P_2 \rangle$ is observed. Molecule polarizations are chaotic within the layers, as indicated by a low value of $\langle m \rangle$ and they are orthogonal to $\hat{\mathbf{n}}$.

A distinct smectic phase is formed over N_{TB} phase for $\chi > 100°$ and over SmA for $\chi \in [140°, 160°]$ [see Fig. 5(e)]. A high value of $\langle m \rangle$ indicates that it is a polar phase and a closer inspection shows that adjacent layers have an opposite (antiferroelectric) polarization. Further analysis reveals that the director $\hat{\mathbf{n}}(x, y, z)$ varies in space. The numerical data is well described by a director field

$$\hat{\mathbf{n}}(x,y,z) = \begin{pmatrix} \sin(\theta)\cos(2\pi z/p) \\ 0 \\ \sqrt{1 - \sin^2(\theta)\cos^2(2\pi z/p)} \end{pmatrix}, \tag{12}$$

thus the phase was identified as splay-bend smectic (Sm_{SB}). The director is constant in xy plane and oscillates within xz plane around $\hat{\mathbf{z}}$ direction, coinciding with the direction $\mathbf{k}$ of density modulation. It is, however, important to note that Sm_{SB} phase emerging in our model is slightly different from the one observed in Ref. [56]. There, the density modulation is non-zero within a whole period and molecules are present between the density maxima [see Fig. 10(a) from Ref. [83]]. On the other hand, in our system, the density is non-zero only near the layer's middle [see Fig. 5(e)] with almost no molecules between the layers. Nonetheless, Eq. (12) holds in the area of non-zero molecule density, thus regarding the phase as Sm_{SB} emphasizes the presence of the director field's modulation.

Although $\hat{\mathbf{n}}(x, y, z)$ leans from $\mathbf{k}$ for a fixed z value, averaging over the whole layer gives $\hat{\mathbf{n}} = 1/p \int_0^p \hat{\mathbf{n}}(x, y, z) dz$ which is parallel to $\mathbf{k}$. Consequently, if one disregards the spatial dependence of the director field and the classification is performed solely on the layer-averaged director and polarization, the phase can be identified as antipolar smectic A ($SmAP_A$) [38,84], observed for V-like shaped hard-core molecules in Ref. [52].

The onset of polar order may be attributed to the entropic gain of translational motion within a layer, however, it does not explain the antiferroelectric arrangement of layer polarization. Lansac *et al.* [52] ascribed such configuration to the more compatible vibrational motion of two molecules from adjacent layers when they have antiparallel directions compared to parallel ones, resulting in once again in a higher entropy of the former system. Sm_{SB}-SmA boundary moves to higher densities for less bent molecules – lower curvatures discourage polar order, so a stronger compression is required to achieve it. In particular, for $\chi > 160°$, a crystallization occurs before the formation of Sm_{SB}[3]. Note that N_{TB} always forms (locally) polar smectic when compressed, which is to be expected since N_{TB} is already (locally) polar.

The director fields (10), (12) are special cases of a more general one [56]:

$$\hat{\mathbf{n}}(x,y,z) = \begin{pmatrix} \sin(\theta_a)\cos(2\pi z/p) \\ \sin(\theta_b)\sin(2\pi z/p) \\ \sqrt{1 - \sin^2(\theta_a)\cos^2(2\pi z/p) - \sin^2(\theta_b)\sin^2(2\pi z/p)} \end{pmatrix}, \tag{13}$$

where the angles θ_a and θ_b may be different. Fixing $\theta_a = \theta$ and continuously changing θ_b from 0 to θ interpolates between director fields for N_{TB} and Sm_{SB}. This intermediate splay-twist-bend smectic (Sm_{STB}) phase has been observed, at present, exclusively for bent spherocylinders [56]. In our model, however, it is absent. One of

[3] Notably, the crystal is polar for $\chi \in [160°, 170°]$ and non-polar above $\chi = 170°$.

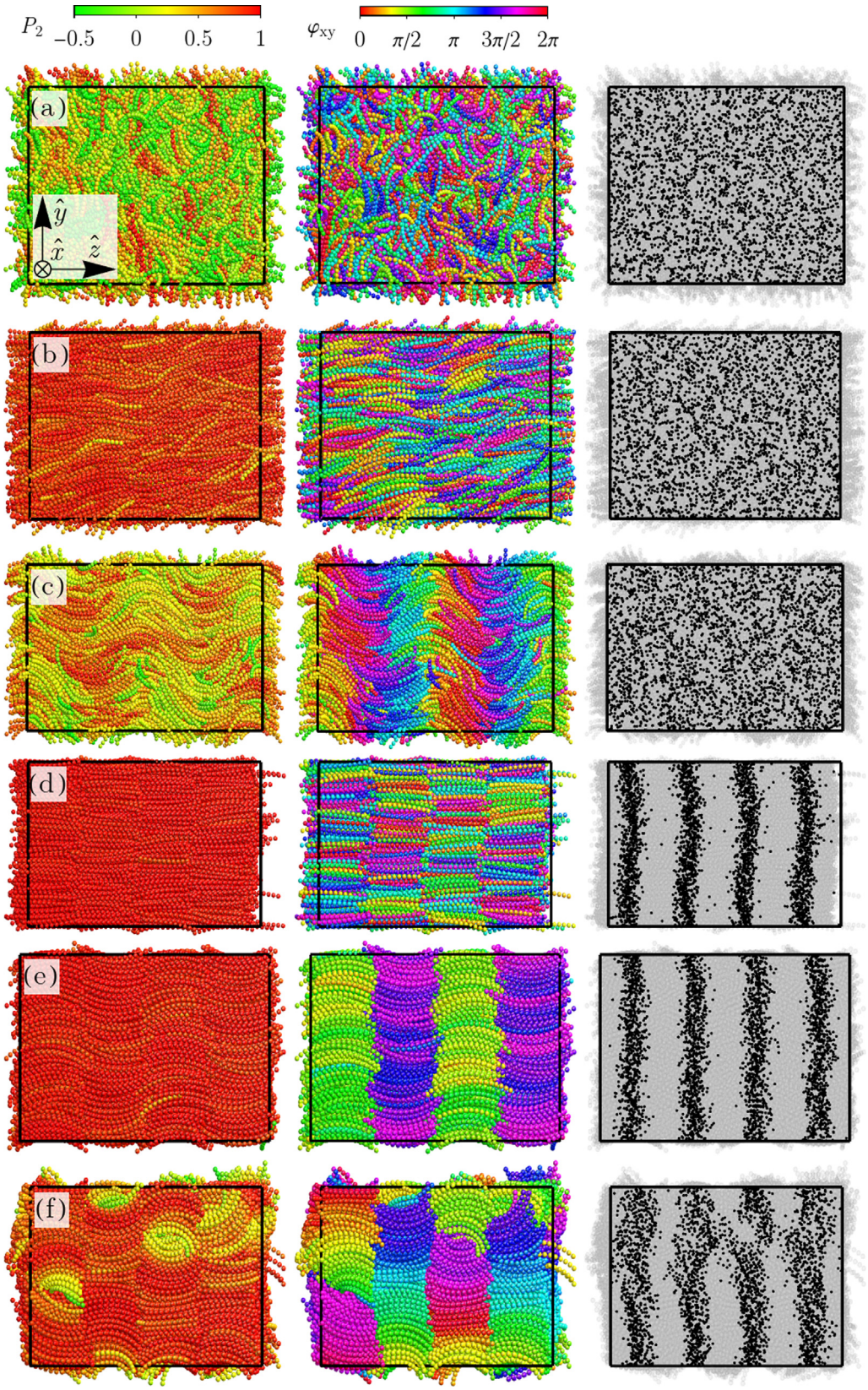

Fig. 5. System snapshots for all identified phases. Each row represents one phase: (a) Iso $[(\chi,\eta)=(95^\circ,0.27)]$, (b) N $[(\chi,\eta)=(140^\circ,0.31)]$, (c) N_{TB} $[(\chi,\eta)=(100^\circ,0.32)]$, (d) SmA $[(\chi,\eta)=(160^\circ,0.39)]$, (e) Sm_{SB} $[(\chi,\eta)=(130^\circ,0.39)]$, (f) SmX $[(\chi,\eta)=(100^\circ,0.41)]$. In the first column molecules are color-coded according to P_2 value, in the second one – according to molecule polarization angle φ_{xy} between x axis and the projection of $\hat{\mathbf{b}}$ onto xy plane. Finally, in the last column, black dots represent molecules' mass centers.

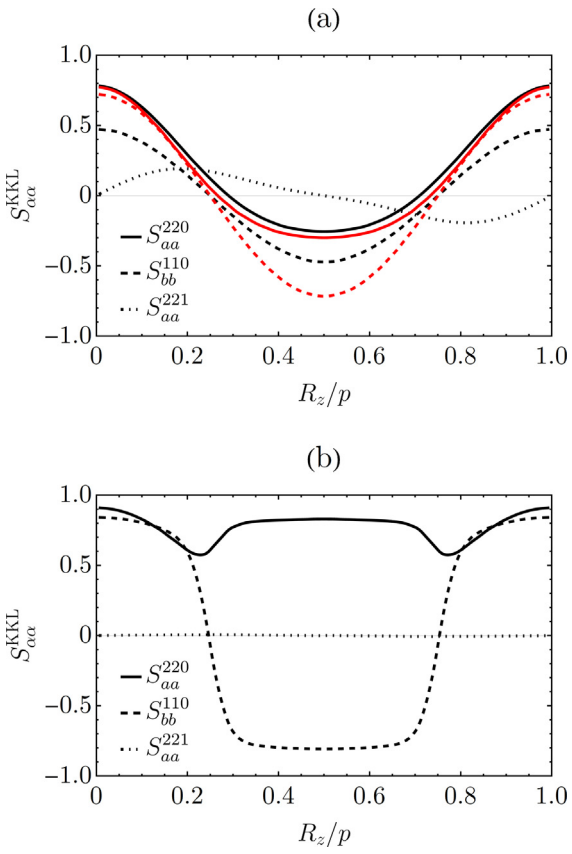

Fig. 6. Pair correlation functions S^{KKL}_{zz} for (a) N_{TB} phase $[(\chi,\eta)=(130^\circ,0.32)$ – black lines and $(\chi,\eta)=(100^\circ,0.33)$ – red lines] and (b) Sm_{SB} phase $[(\chi,\eta)=(115^\circ,0.37)]$. Solid, dashed and dotted lines correspond to, respectively, S^{220}_{aa}, S^{110}_{bb} and S^{221}_{aa}. S^{221}_{aa} parameter for $(\chi,\eta)=(100^\circ,0.33)$ is not shown, since it overlaps with the one for $(\chi,\eta)=(130^\circ,0.32)$. The distance R_z is given in units of the structure's period (for Sm_{SB} it is a width of two layers).

the reasons might be the length of the molecules (ours are shorter than in Ref. [56]) or undulated surface created by beads (contrary to a smooth one in Ref. [56]), which hinders sliding of the molecules along themselves.

Correlation functions for $(\chi,\eta)=(115^\circ,0.37)$ are shown in Fig. 6(b). Here, due to the antiferroelectric arrangement, the period p is the width of two layers. Nematic-like correlations measured by S^{220}_{aa} are high in a whole range with two shallow minima around $R_z=p/4$ and $R_z=3p/4$. These R_z values are the distances between a middle of a layer and a space between layers, where molecules are very scarce and less ordered, which as a result lowers S^{220}_{aa}. A lower value for $R_z=p/2$ when compared to $R_z=0,p$ may be attributed to splay-bend modulation of the director field (12) – although the directors in the middle of adjacent, antipolar layers are parallel, away from the middle, the director tilts in a different direction. S^{110}_{bb} reaches 0.8 for $R_z\in[0,0.2p]$ and $R_z\in[0.8p,p]$, representing the high correlations of polarization within the layer and two layers further, respectively, while for $R_z\in[0.3p,0.7p]$, S^{110}_{bb} is equal to -0.8 confirming anti-correlations in adjacent layers. Since the structure is achiral, S^{221}_{aa} is zero in the whole range of R_z.

Highly bent molecules form yet another polar smectic phase, as indicated by high $\langle\tau\rangle$ and $\langle m\rangle$ values, however of an unknown type, thus denoted as SmX [see Fig. 5(f)]. Despite trying both compression and expansion from various initial configurations (dense crystal, diluted crystal, type C smectic, lower-density equilibrium system, and others), as well as relaxation in a triclinic simulation box, where both the side lengths and the angles between the box faces are allowed to change, we were not able to obtain a structure without irregular domain walls. As it can be seen from Fig. 5, the polarization within each stratus rotates with y coordinate and topological defects are visible. The same effects are present for both hard and soft interactions. Increasing the system size, which allows a full rotation of the molecule polarization vector has not eliminated the defects and in neither case they form a regular pattern as in, e.g., blue phases [85]. However, the blue-phase-like structures cannot be completely disregarded since the lattice constant of the defects can be of the order of tens or even hundreds of molecule lengths, and the system size allowing such long periods is far beyond the limit of our computational resources. Another candidate is anticlinic, antiferroelectric type C smectic (SmC_AP_A) [38,84]. There, both the director tilt and polarization alternate between layers. Remarkably, we have observed its formation for a very acute bend angle $\chi<70^\circ$ and a high density $\eta>0.4$ (see Fig. 7).

BSMs with highly acute bend angles are still scarce and not fully understood [84,86]. Chemical data indicate that increasing the mesogens' degree of bend decreases the LC phase stability, which leads to a loss of mesogenic properties [87]. Therefore, $\chi<90^\circ$ falls outside of the scope of this work. Nevertheless, further investigation of the unidentified SmX phase can be a potential goal for future studies.

Our simulation results correlate well with the experimentally observed phase sequences for BSMs [88,16,89]. Additionally, the mapped region of N_{TB}'s stability, governed by the bend angle, is in fairly good agreement with the empirical data [90,17,91].

The studied system undergoes following phase transitions:

a) Iso ↔ N ↔ SmA,
b) Iso ↔ N ↔ SmA ↔ Sm_{SB},
c) Iso ↔ N ↔ N_{TB} ↔ Sm_{SB},
d) Iso ↔ N ↔ N_{TB} ↔ Sm_{SB} ↔ SmX,
e) Iso ↔ N_{TB} ↔ Sm_{SB} ↔ SmX,
f) Iso ↔ N_{TB} ↔ SmX.

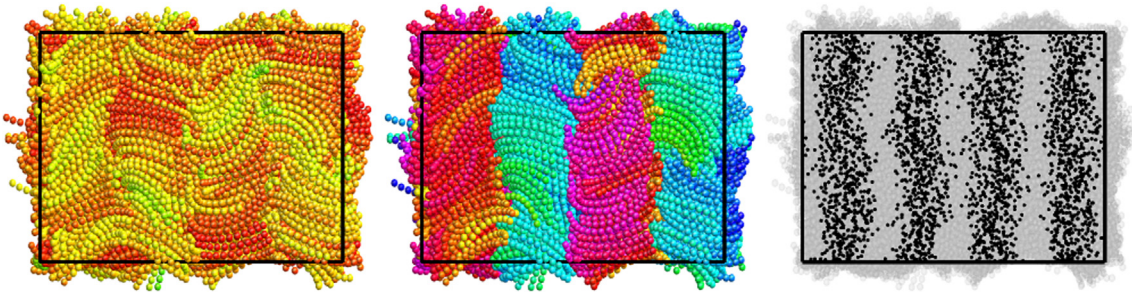

Fig. 7. System snapshot for SmC_AP_A phase $[(\chi,\eta)=(65^\circ,0.45)]$ in analogy to Fig. 5.

Sequence (a) is quite common in systems composed of BSMs [89] in contrary to sequences (b-f). As far as we know, in the literature are reported only variants of twist-bend smectic phase [92,93] without any mentions of splay-bend smectic. What is more, the compounds that form N_{TB} directly from Iso are uncommon [88]. On the other hand, there are some premises that SmX might be one of smectic phases outlined in [94,95]. For the CB6O.S*m* series ($m = 13, 15, 17$) following phase sequence was found [96]: Iso $\leftrightarrow$ N $\leftrightarrow$ SmA $\leftrightarrow$ SmX $\leftrightarrow$ SmC_{TB}, which is similar to sequence (b).

At this point, it is worth emphasizing the fact that the twist-bend nematic phase was identified exclusively in thermotropic systems, whereas the splay-bend nematic (N_{SB}) solely in colloidal systems of "banana-shaped" particles [23] and bent silica rods [97]. The discovery of thermotropic N_{SB} and N_B, along with lyotropic N_{TB} [98], will constitute the next key milestones on the roadmap of liquid crystal science.

4. Conclusions

We have systematically studied the phase diagram of the liquids formed by bent-shaped molecules composed of tangential spheres with centers placed on an arc. The molecules were described by adjustable bend angle χ and the system composed of such molecules was considered under different packing fractions η. In (χ, η) parameters space, we have identified following phases: isotropic, nematic, twist-bend nematic, smectic A, and splay-bend smectic. For the highest density and the largest χ we have observed a smectic phase, denoted as SmX, forming polar layers with in-layer rotating polarization. We were, however, not able to avoid defects and domain walls. For unrealistically large bend, SmX phase transformed to anticlinic, antiferroelectric type C smectic, where both the director tilt and polarization alternate between layers. In comparison to a previous study for bent spherocylinders [56], we have not observed splay-twist-bend smectic. The obtained results were the same for both: MC with hard-core interactions and MD using short-range WCA repulsion.

Data availability

The datasets generated during and/or analyzed during the current study are available from P.K. and W.T. upon reasonable request.

Code availability

The source code of an original simulation package used to perform Monte Carlo sampling is available at https://github.com/PKua007/rampack. Input script for LAMMPS is available from W. T. upon reasonable request.

Author Contributions

P.K.: conceptualization, data curation, formal analysis, funding acquisition, investigation, project administration, software, visualization, writing. W.T.: conceptualization, data curation, formal analysis, investigation, validation, visualization, writing. M.C.: conceptualization, writing.

Declaration of Competing Interest

The authors declare that they have no known competing financial interests or personal relationships that could have appeared to influence the work reported in this paper.

Acknowledgements

P.K. acknowledges the support of Ministry of Science and Higher Education (Poland) Grant No. 0108/DIA/2020/49. W.T. was funded by the statutory activity of the Jerzy Haber Institute of Catalysis and Surface Chemistry, Polish Academy of Sciences. M. C. acknowledges the support of National Science Centre in Poland Grant No. 2021/43/B/ST3/03135. We are thankful to prof. Lech Longa for fruitful and insightful discussions. Numerical simulations were carried out with the support of the Interdisciplinary Center for Mathematical and Computational Modelling (ICM) at the University of Warsaw under Grant No. GB76-1.

References

[1] N. Fujii, T. Saito, Homochirality and life, Chem. Record 4 (2004) 267–278, https://doi.org/10.1002/tcr.20020.
[2] C. Viedma, Chiral symmetry breaking and complete chiral purity by thermodynamic-kinetic feedback near equilibrium: implications for the origin of biochirality, Astrobiol. 7 (2007) 312–319, https://doi.org/10.1089/ast.2006.0099.
[3] K. Ruiz-Mirazo, C. Briones, A. de la Escosura, Prebiotic Systems Chemistry: New Perspectives for the Origins of Life, Chem. Rev. 114 (2014) 285–366, https://doi.org/10.1021/cr2004844.
[4] E. Yashima, N. Ousaka, D. Taura, K. Shimomura, T. Ikai, K. Maeda, Supramolecular helical systems: Helical assemblies of small molecules, foldamers, and polymers with chiral amplification and their functions, Chem. Rev. 116 (2016) 13752–13990, https://doi.org/10.1021/acs.chemrev.6b00354.
[5] Y. Sang, M. Liu, Hierarchical self-assembly into chiral nanostructures, Chem. Sci. 13 (2022) 633–656, https://doi.org/10.1039/D1SC03561D.
[6] G. Heppke, D. Moro, Chiral order from achiral molecules, Science 279 (1998) 1872–1873, https://doi.org/10.1126/science.279.5358.1872.
[7] C. Tschierske, Mirror symmetry breaking in liquids and liquid crystals, Liq. Cryst. 45 (2018) 2221–2252, https://doi.org/10.1080/02678292.2018.1501822.
[8] C. Zhang, N. Diorio, O.D. Lavrentovich, A. Jákli, Helical nanofilaments of bent-core liquid crystals with a second twist, Nat. Commun. 5 (2014) 3302, https://doi.org/10.1038/ncomms4302.
[9] A. Jákli, O.D. Lavrentovich, J.V. Selinger, Physics of liquid crystals of bent-shaped molecules, Rev. Mod. Phys. 90 (2018) 045004, https://doi.org/10.1103/RevModPhys.90.045004.
[10] L. Li, M. Salamończyk, S. Shadpour, C. Zhu, A. Jákli, T. Hegmann, An unusual type of polymorphism in a liquid crystal, Nat. Commun. 9 (2018) 714, https://doi.org/10.1038/s41467-018-03160-9.
[11] M. Cestari, S. Diez-Berart, D.A. Dunmur, A. Ferrarini, M.R. de la Fuente, D.J.B. Jackson, D.O. Lopez, G.R. Luckhurst, M.A. Perez-Jubindo, R.M. Richardson, J. Salud, B.A. Timimi, H. Zimmermann, Phase behavior and properties of the liquid-crystal dimer 1",7"-bis(4-cyanobiphenyl-4'-yl) heptane: A twist-bend nematic liquid crystal, Phys. Rev. E 84 (2011) 031704, https://doi.org/10.1103/PhysRevE.84.031704.
[12] V. Borshch, Y.-K. Kim, J. Xiang, M. Gao, A. Jákli, V.P. Panov, J.K. Vij, C.T. Imrie, M. G. Tamba, G.H. Mehl, O.D. Lavrentovich, Nematic twist-bend phase with nanoscale modulation of molecular orientation, Nat. Commun. 4 (2013) 2635, https://doi.org/10.1038/ncomms3635.
[13] D. Chen, J.H. Porada, J.B. Hooper, A. Klittnick, Y. Shen, M.R. Tuchband, E. Korblova, D. Bedrov, D.M. Walba, M.A. Glaser, J.E. Maclennan, N.A. Clark, Chiral heliconical ground state of nanoscale pitch in a nematic liquid crystal of achiral molecular dimers, Proc. Natl. Acad. Sci. U.S.A. 110 (2013) 15931–15936, https://doi.org/10.1073/pnas.1314654110.
[14] G. D'Alessandro, G.R. Luckhurst, T.J. Sluckin, Twist-bend nematics and beyond, Liq. Cryst. 44 (2017) 1–3, https://doi.org/10.1080/02678292.2017.1288698.
[15] R. Mandle, E. Davis, C.-C. Voll, C. Archbold, J. Goodby, S. Cowling, The relationship between molecular structure and the incidence of the NTB phase, Liq. Cryst. 42 (2015) 688–703, https://doi.org/10.1080/02678292.2014.974698.
[16] R.J. Mandle, The dependency of twist-bend nematic liquid crystals on molecular structure: a progression from dimers to trimers, oligomers and polymers, Soft Matter 12 (2016) 7883–7901, https://doi.org/10.1039/C6SM01772J.
[17] R.J. Mandle, C.T. Archbold, J.P. Sarju, J.L. Andrews, J.W. Goodby, The dependency of nematic and twist-bend mesophase formation on bend angle, Sci. Rep. 6 (2016) 36682, https://doi.org/10.1038/srep36682.
[18] R.B. Meyer, Structural problems in liquid crystal physics, in: R. Balian, G. Weill (Eds.), Molecular Fluids, Proceedings of the Les Houches Summer School on Theoretical Physics, 1973, session No. XXV, Gordon and Breach Science Publishers, 1976, p. 271.
[19] I. Dozov, On the spontaneous symmetry breaking in the mesophases of achiral banana-shaped molecules, Europhysics Letters (EPL) 56 (2001) 247–253, https://doi.org/10.1209/epl/i2001-00513-x.

[20] E.T. Samulski, A.G. Vanakaras, D.J. Photinos, The twist bend nematic: a case of mistaken identity, Liq. Cryst. 47 (2020) 2092–2097, https://doi.org/10.1080/02678292.2020.1795943.
[21] I. Dozov, G.R. Luckhurst, Setting things straight in 'The twist-bend nematic: a case of mistaken identity', Liq. Cryst. 47 (2020) 2098–2115, https://doi.org/10.1080/02678292.2020.1795944.
[22] C. Meyer, C. Blanc, G.R. Luckhurst, P. Davidson, I. Dozov, Biaxiality-driven twist-bend to splay-bend nematic phase transition induced by an electric field, Sci. Adv. 6 (2020) eabb8212, https://doi.org/10.1126/sciadv.abb8212.
[23] C. Fernández-Rico, M. Chiappini, T. Yanagishima, H. de Sousa, D.G.A.L. Aarts, M. Dijkstra, R.P.A. Dullens, Shaping colloidal bananas to reveal biaxial, splay-bend nematic, and smectic phases, Science 369 (2020) 950–955, https://doi.org/10.1126/science.abb4536.
[24] R.J. Mandle, N. Sebastián, J. Martinez-Perdiguero, A. Mertelj, On the molecular origins of the ferroelectric splay nematic phase, Nat. Commun. 12 (2021) 4962, https://doi.org/10.1038/s41467-021-25231-0.
[25] N. Sebastián, M. Čopič, A. Mertelj, Ferroelectric nematic liquid-crystalline phases, Phys. Rev. E 106 (2022), https://doi.org/10.1103/PhysRevE.106.021001 021001.
[26] J.W. Emsley, M. Lelli, A. Lesage, G.R. Luckhurst, A Comparison of the Conformational Distributions of the Achiral Symmetric Liquid Crystal Dimer CB7CB in the Achiral Nematic and Chiral Twist-Bend Nematic Phases, J. Phys. Chem. B 117 (2013) 6547–6557, https://doi.org/10.1021/jp4001219.
[27] W. Tomczyk, L. Longa, Role of molecular bend angle and biaxiality in the stabilization of the twist-bend nematic phase, Soft Matter 16 (2020) 4350–4357, https://doi.org/10.1039/D0SM00078G.
[28] L. Longa, W. Tomczyk, Twist-Bend Nematic Phase from the Landau–de Gennes Perspective, J. Phys. Chem. C 124 (2020) 22761–22775, https://doi.org/10.1021/acs.jpcc.0c05711.
[29] H. Takezoe, A. Eremin, Peculiarities of the N phases, in: Bent-Shaped Liquid Crystals: Structures and Physical Properties, 1 ed., CRC Press, 2017, pp. 117–168.
[30] M.J. Freiser, Ordered states of a nematic liquid, Phys. Rev. Lett. 24 (1970) 1041–1043, https://doi.org/10.1103/PhysRevLett.24.1041.
[31] M. Mathews, S. Kang, S. Kumar, Q. Li, Designing bent-core nematogens towards biaxial nematic liquid crystals, Liq. Cryst. 38 (2011) 31–40, https://doi.org/10.1080/02678292.2010.524716.
[32] M. Lehmann, Low molar mass thermotropic systems, in: Biaxial Nematic Liquid Crystals, John Wiley & Sons Ltd, 2015, pp. 333–367. doi: 10.1002/9781118696316.ch14.
[33] T.C. Lubensky, L. Radzihovsky, Theory of bent-core liquid-crystal phases and phase transitions, Phys. Rev. E 66 (2002) 031704, https://doi.org/10.1103/PhysRevE.66.031704.
[34] B. Mettout, Theory of uniaxial and biaxial nematic phases in bent-core systems, Phys. Rev. E 72 (2005) 031706, https://doi.org/10.1103/PhysRevE.72.031706.
[35] M.B. Ros, J.L. Serrano, M.R. de la Fuente, C.L. Folcia, Banana-shaped liquid crystals: a new field to explore, J. Mater. Chem. 15 (2005) 5093–5098, https://doi.org/10.1039/B504384K.
[36] B. Mettout, Theory of two- and three-dimensional bent-core mesophases, Phys. Rev. E 75 (2007) 011706, https://doi.org/10.1103/PhysRevE.75.011706.
[37] W. Tomczyk, G. Pająk, L. Longa, Twist-bend nematic phases of bent-shaped biaxial molecules, Soft Matter 12 (2016) 7445–7452, https://doi.org/10.1039/C6SM01197G.
[38] R.A. Reddy, C. Tschierske, Bent-core liquid crystals: polar order, superstructural chirality and spontaneous desymmetrisation in soft matter systems, J. Mater. Chem. 16 (2006) 907–961, https://doi.org/10.1039/B504400F.
[39] A. Eremin, A. Jákli, Polar bent-shape liquid crystals – from molecular bend to layer splay and chirality, Soft Matter 9 (2013) 615–637, https://doi.org/10.1039/C2SM26780B.
[40] C.M. Care, D.J. Cleaver, Computer simulation of liquid crystals, Rep. Prog. Phys. 68 (2005) 2665–2700, https://doi.org/10.1088/0034-4885/68/11/r04.
[41] M.R. Wilson, Progress in computer simulations of liquid crystals, Int. Rev. Phys. Chem. 24 (2005) 421–455, https://doi.org/10.1080/01442350500361244.
[42] M.P. Allen, Molecular simulation of liquid crystals, Mol. Phys. 117 (2019) 2391–2417, https://doi.org/10.1080/00268976.2019.1612957.
[43] R. Tavarone, P. Charbonneau, H. Stark, Phase ordering of zig-zag and bow-shaped hard needles in two dimensions, J. Chem. Phys. 143 (2015) 114505, https://doi.org/10.1063/1.4930886.
[44] P. Karbowniczek, M. Cieśla, L. Longa, A. Chrzanowska, Structure formation in monolayers composed of hard bent-core molecules, Liq. Cryst. 44 (2017) 254–272, https://doi.org/10.1080/02678292.2016.1259510.
[45] J.P. Ramírez González, G. Cinacchi, Phase behavior of hard circular arcs, Phys. Rev. E 104 (2021) 054604, https://doi.org/10.1103/PhysRevE.104.054604.
[46] J. Xu, R.L.B. Selinger, J.V. Selinger, R. Shashidhar, Monte Carlo simulation of liquid-crystal alignment and chiral symmetry-breaking, J. Chem. Phys. 115 (2001) 4333–4338, https://doi.org/10.1063/1.1389857.
[47] A. Dewar, P.J. Camp, Computer simulations of bent-core liquid crystals, Phys. Rev. E 70 (2004) 011704, https://doi.org/10.1103/PhysRevE.70.011704.
[48] P. De Gregorio, E. Frezza, C. Greco, A. Ferrarini, Density functional theory of nematic elasticity: softening from the polar order, Soft Matter 12 (2016) 5188–5198, https://doi.org/10.1039/C6SM00624H.
[49] C. Greco, A. Ferrarini, Entropy-driven chiral order in a system of achiral bent particles, Phys. Rev. Lett. 115 (2015) 147801, https://doi.org/10.1103/PhysRevLett.115.147801.
[50] T. Drwenski, S. Dussi, M. Dijkstra, R. van Roij, P. van der Schoot, Connectedness percolation of hard deformed rods, J. Chem. Phys. 147 (2017) 224904, https://doi.org/10.1063/1.5006380.
[51] P.J. Camp, M.P. Allen, A.J. Masters, Theory and computer simulation of bent-core molecules, J. Chem. Phys. 111 (1999) 9871–9881, https://doi.org/10.1063/1.480324.
[52] Y. Lansac, P.K. Maiti, N.A. Clark, M.A. Glaser, Phase behavior of bent-core molecules, Phys. Rev. E 67 (2003) 011703, https://doi.org/10.1103/PhysRevE.67.011703.
[53] S.D. Peroukidis, A.G. Vanakaras, D.J. Photinos, Molecular simulation of hierarchical structures in bent-core nematic liquid crystals, Phys. Rev. E 84 (2011) 010702, https://doi.org/10.1103/PhysRevE.84.010702.
[54] S.D. Peroukidis, A.G. Vanakaras, D.J. Photinos, Molecular simulation study of polar order in orthogonal bent-core smectic liquid crystals, Phys. Rev. E 91 (2015) 062501, https://doi.org/10.1103/PhysRevE.91.062501.
[55] M. Chiappini, T. Drwenski, R. van Roij, M. Dijkstra, Biaxial, Twist-bend, and Splay-bend Nematic Phases of Banana-shaped Particles Revealed by Lifting the "Smectic Blanket", Phys. Rev. Lett. 123 (2019) 068001, https://doi.org/10.1103/PhysRevLett.123.068001.
[56] M. Chiappini, M. Dijkstra, A generalized density-modulated twist-splay-bend phase of banana-shaped particles, Nat. Commun. 12 (2021) 2157, https://doi.org/10.1038/s41467-021-22413-8.
[57] S. Dussi, M. Dijkstra, Entropy-driven formation of chiral nematic phases by computer simulations, Nat. Commun. 7 (2016) 11175, https://doi.org/10.1038/ncomms11175.
[58] R. Memmer, Liquid crystal phases of achiral banana-shaped molecules: a computer simulation study, Liq. Cryst. 29 (2002) 483–496, https://doi.org/10.1080/02678290110104586.
[59] S.M. Shamid, S. Dhakal, J.V. Selinger, Statistical mechanics of bend flexoelectricity and the twist-bend phase in bent-core liquid crystals, Phys. Rev. E 87 (2013) 052503, https://doi.org/10.1103/PhysRevE.87.052503.
[60] A.G. Vanakaras, D.J. Photinos, Molecular dynamics simulations of nematic phases formed by cyano-biphenyl dimers, Liq. Cryst. 45 (2018) 2184–2196, https://doi.org/10.1080/02678292.2018.1528639.
[61] J. Shi, H. Sidky, J.K. Whitmer, Novel elastic response in twist-bend nematic models, Soft Matter 15 (2019) 8219–8226, https://doi.org/10.1039/C9SM01395D.
[62] G. Yu, M.R. Wilson, All-atom simulations of bent liquid crystal dimers: the twist-bend nematic phase and insights into conformational chirality, Soft Matter 18 (2022) 3087–3096, https://doi.org/10.1039/D2SM00291D.
[63] M. Tarini, P. Cignoni, C. Montani, Ambient occlusion and edge cueing for enhancing real time molecular visualization, IEEE Trans. Vis. Comput. Graph. 12 (2006) 1237–1244, https://doi.org/10.1109/TVCG.2006.115.
[64] L. Mederos, E. Velasco, Y. Martínez-Ratón, Hard-body models of bulk liquid crystals, J. Phys. Condens. Matter 26 (2014) 463101, https://doi.org/10.1088/0953-8984/26/46/463101.
[65] J.D. Weeks, D. Chandler, H.C. Andersen, Role of repulsive forces in determining the equilibrium structure of simple liquids, J. Chem. Phys. 54 (1971) 5237–5247, https://doi.org/10.1063/1.1674820.
[66] D. Chandler, J.D. Weeks, H.C. Andersen, Van der waals picture of liquids, solids, and phase transformations, Science 220 (1983) 787–794, https://doi.org/10.1126/science.220.4599.787.
[67] D. Frenkel, Computer simulation of hard-core models for liquid crystals, Mol. Phys. 60 (1987) 1–20, https://doi.org/10.1080/00268978700100011.
[68] D.M. Heyes, H. Okumura, Equation of state and structural properties of the Weeks-Chandler-Andersen fluid, J. Chem. Phys. 124 (2006) 164507, https://doi.org/10.1063/1.2176675.
[69] W.W. Wood, Monte Carlo studies of simple liquid models, in: H.N.V. Temperley, J.S. Rowlinson, G.S. Rushbrooke (Eds.), Physics of simple liquids, North-Holland, 1968.
[70] J.A. Anderson, M.E. Irrgang, S.C. Glotzer, Scalable Metropolis Monte Carlo for simulation of hard shapes, Comp. Phys. Commun. 204 (2016) 21–30, https://doi.org/10.1016/j.cpc.2016.02.024.
[71] A.P. Thompson, H.M. Aktulga, R. Berger, D.S. Bolintineanu, W.M. Brown, P.S. Crozier, P.J. in 't Veld, A. Kohlmeyer, S.G. Moore, T.D. Nguyen, R. Shan, M.J. Stevens, J. Tranchida, C. Trott, S.J. Plimpton, LAMMPS - a flexible simulation tool for particle-based materials modeling at the atomic, meso, and continuum scales, Comp. Phys. Comm. 271 (2022) 108171, https://doi.org/10.1016/j.cpc.2021.108171.
[72] C. Greco, A. Ferrarini, 2015. See Supplemental Material of [Phys. Rev. Lett. 115, 147801 (2015)], which is available at: https://journals.aps.org/prl/supplemental/10.1103/PhysRevLett.115.147801/greco_SM.pdf.
[73] P.G. de Gennes, J. Prost, The Physics of Liquid Crystals, 2 ed., Clarendon Press, 1993.
[74] R. Eppenga, D. Frenkel, Monte Carlo study of the isotropic and nematic phases of infinitely thin hard platelets, Mol. Phys. 52 (1984) 1303–1334, https://doi.org/10.1080/00268978400101951.
[75] W.H. De Jeu, Basic X-ray scattering for soft matter, Oxford University Press, 2016.
[76] A.J. Stone, The description of bimolecular potentials, forces and torques: the S and V function expansions, Mol. Phys. 36 (1978) 241–256, https://doi.org/10.1080/00268977800101541.
[77] S. Chandrasekhar, N.V. Madhusudana, Liquid crystals, Annu. Rev. Mater. Sci. 10 (1980) 133–155, https://doi.org/10.1146/annurev.ms.10.080180.001025.
[78] C.W. Oseen, The theory of liquid crystals, Trans. Faraday Soc. 29 (1933) 883–899, https://doi.org/10.1039/TF9332900883.

[79] H. Zocher, The effect of a magnetic field on the nematic state, Trans. Faraday Soc. 29 (1933) 945–957, https://doi.org/10.1039/TF9332900945.
[80] F.C. Frank, I. liquid crystals. on the theory of liquid crystals, Discuss. Faraday Soc. 25 (1958) 19–28, https://doi.org/10.1039/DF9582500019.
[81] J.L. Ericksen, Inequalities in liquid crystal theory, Phys. Fluids 9 (1966) 1205–1207, https://doi.org/10.1063/1.1761821.
[82] L. Longa, G. Pająk, Modulated nematic structures induced by chirality and steric polarization, Phys. Rev. E 93 (2016) 040701, https://doi.org/10.1103/PhysRevE.93.040701.
[83] M. Chiappini, M. Dijkstra, 2021. See Supplemental Material of [Nat. Comm. 12, 2157 (2021)], which is available at: https://static-content.springer.com/esm/art%3A10.1038%2Fs41467-021-22413-8/MediaObjects/41467_2021_22413_MOESM1_ESM.pdf.
[84] N. Gimeno, M. Blanca Ros, Chemical structures, mesogenic properties, and synthesis of liquid crystals with bent-core structures, in: Handbook of Liquid Crystals, John Wiley & Sons Ltd, 2014, pp. 1–75. DOI:10.1002/9783527671403.hlc070.
[85] D.C. Wright, N.D. Mermin, Crystalline liquids: the blue phases, Rev. Mod. Phys. 61 (1989) 385–432, https://doi.org/10.1103/RevModPhys.61.385.
[86] H. Takezoe, A. Eremin, Phase structures, in: Bent-Shaped Liquid Crystals: Structures and Physical Properties, 1 ed., CRC Press, 2017, pp. 39–116.
[87] M. Hird, Banana-shaped and other bent-core liquid crystals, Liq. Cryst. Today 14 (2005) 9–21, https://doi.org/10.1080/14645180500274347.
[88] A.A. Dawood, M.C. Grossel, G.R. Luckhurst, R.M. Richardson, B.A. Timimi, N.J. Wells, Y.Z. Yousif, On the twist-bend nematic phase formed directly from the isotropic phase, Liq. Cryst. 43 (2016) 2–12, https://doi.org/10.1080/02678292.2015.1114158.
[89] S. Kumar, S.K. Pal, Liquid Crystal Dimers, Cambridge University Press, 2017, https://doi.org/10.1017/9781316662120.
[90] C. Zhu, M.R. Tuchband, A. Young, M. Shuai, A. Scarbrough, D.M. Walba, J.E. Maclennan, C. Wang, A. Hexemer, N.A. Clark, Resonant Carbon K-Edge Soft X-Ray Scattering from Lattice-Free Heliconical Molecular Ordering: Soft Dilative Elasticity of the Twist-Bend Liquid Crystal Phase, Phys. Rev. Lett. 116 (2016) 147803, https://doi.org/10.1103/PhysRevLett.116.147803.
[91] E. Cruickshank, M. Salamonczyk, D. Pociecha, G.J. Strachan, J.M.D. Storey, C. Wang, J. Feng, C. Zhu, E. Gorecka, C.T. Imrie, Sulfur-linked cyanobiphenyl-based liquid crystal dimers and the twist-bend nematic phase, Liq. Cryst. 46 (2019) 1595–1609, https://doi.org/10.1080/02678292.2019.1641638.
[92] J.P. Abberley, R. Killah, R. Walker, J.M.D. Storey, C.T. Imrie, M. Salamończyk, C. Zhu, E. Gorecka, D. Pociecha, Heliconical smectic phases formed by achiral molecules, Nat. Commun. 9 (2018) 228, https://doi.org/10.1038/s41467-017-02626-6.
[93] A.F. Alshammari, D. Pociecha, R. Walker, J.M.D. Storey, E. Gorecka, C.T. Imrie, New patterns of twist-bend liquid crystal phase behaviour: the synthesis and characterisation of the 1-(4-cyanobiphenyl-4'-yl)-10-(4-alkylaniline-benzylidene-4'-oxy)decanes (CB10Om), Soft Matter (2022), https://doi.org/10.1039/D2SM00162D.
[94] S.P. Sreenilayam, Y.P. Panarin, J.K. Vij, V.P. Panov, A. Lehmann, M. Poppe, M. Prehm, C. Tschierske, Spontaneous helix formation in non-chiral bent-core liquid crystals with fast linear electro-optic effect, Nat. Commun. 7 (2016) 11369, https://doi.org/10.1038/ncomms11369.
[95] A. Lehmann, M. Alaasar, M. Poppe, S. Poppe, M. Prehm, M. Nagaraj, S.P. Sreenilayam, Y.P. Panarin, J.K. Vij, C. Tschierske, Stereochemical rules govern the soft self-assembly of achiral compounds: Understanding the heliconical liquid-crystalline phases of bent-core mesogens, Chemistry – A, European Journal 26 (2020) 4714–4733, https://doi.org/10.1002/chem.201904871.
[96] E. Cruickshank, K. Anderson, J. Storey, C. Imrie, E. Gorecka, D. Pociecha, A. Makal, M. Majewska, Helical phases assembled from achiral molecules: Twist-bend nematic and helical filamentary B4 phases formed by mesogenic dimers, J. Mol. Liq. 346 (2022) 118180, https://doi.org/10.1016/j.molliq.2021.118180.
[97] R. Kotni, A. Grau-Carbonell, M. Chiappini, M. Dijkstra, A. van Blaaderen, Splay-bend nematic phases of bent colloidal silica rods induced by polydispersity, PREPRINT (Version 1) available at Research Square [https://doi.org/10.21203/rs.3.rs-1594517/v1], 2022.
[98] C. Anzivino, R. van Roij, M. Dijkstra, A Landau–de Gennes theory for twist-bend and splay-bend nematic phases of colloidal suspensions of bent rods, J. Chem. Phys. 152 (2020) 224502, https://doi.org/10.1063/5.0008936.